Plasma spectroscopy when there is magnetic reconnection associated with Rayleigh-Taylor instability in the Caltech spheromak jet experiment

KB Chai
Korea Atomic Energy Research Institute/Caltech

Paul M. Bellan
Caltech

Caltech spheromak jet experiment

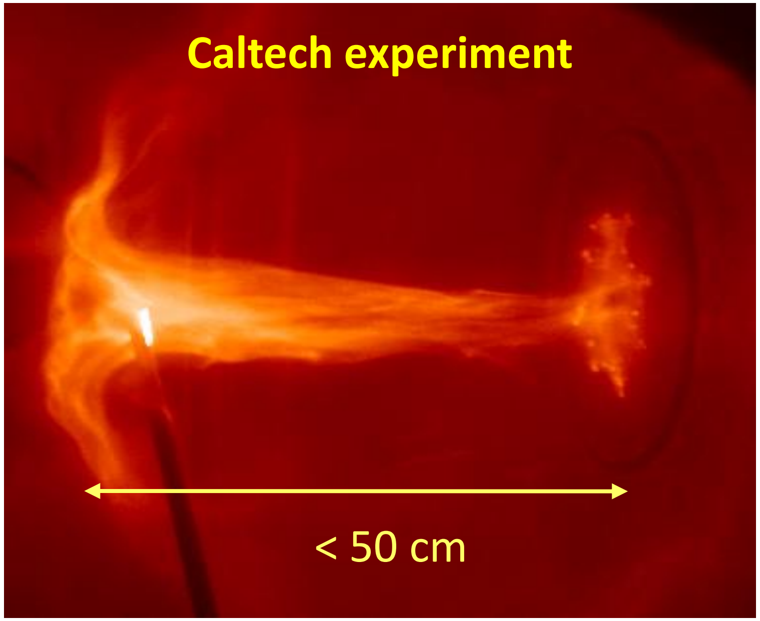

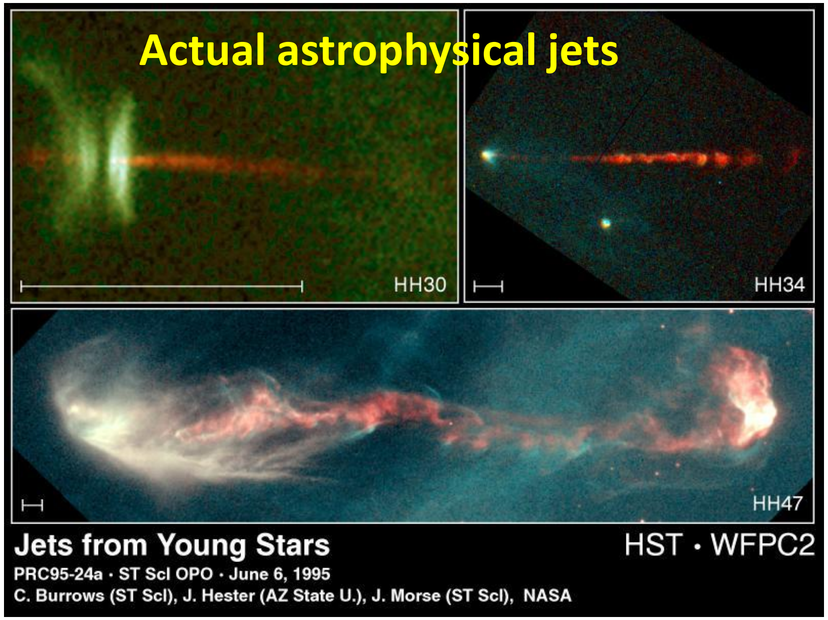

- **Simulate non-relativistic astrophysical jets in the laboratory**
  - Astrophysical jets: plasma outflows from heavy objects
  - Typical size: 200 – 2000 AU

Dimensionless nature of MHD

Dimensionless MHD equations

$$\frac{\partial \bar{\rho}}{\partial \tau} + \bar{\nabla} \cdot (\bar{\rho} \bar{\mathbf{U}}) = 0$$: Continuity eq.

$$\bar{\rho}\left(\frac{\partial}{\partial \tau} + \bar{\mathbf{U}} \cdot \bar{\nabla}\right)\bar{\mathbf{U}} = \bar{\mathbf{J}} \times \bar{\mathbf{B}} - \bar{\nabla}\mathbf{P}$$: Eq. of motion

$$\bar{\nabla} \times \bar{\mathbf{B}} = \bar{\mathbf{J}}$$: Ampere’s law

$$\frac{\partial \bar{\mathbf{B}}}{\partial \tau} = \bar{\nabla} \times (\bar{\mathbf{U}} \times \bar{\mathbf{B}}) + \cancelto{}{\frac{1}{S}\bar{\nabla}^2 \bar{\mathbf{B}}}$$: Induction eq.

- Lundquist number: $S = \mu_0 L v_A/\eta$, Alfven speed: $v_A = B/(\rho\mu)^{1/2}$
  - Astrophysical jets: $S = 10^{10}$-10^{20}
  - Solar corona loops: $S \geq 10^{12}$
  - Tokamaks: $S = 10^8$
  - Caltech jet: $S = 10$-100

➡ **Same equations, same physics**

Magnetic reconnection

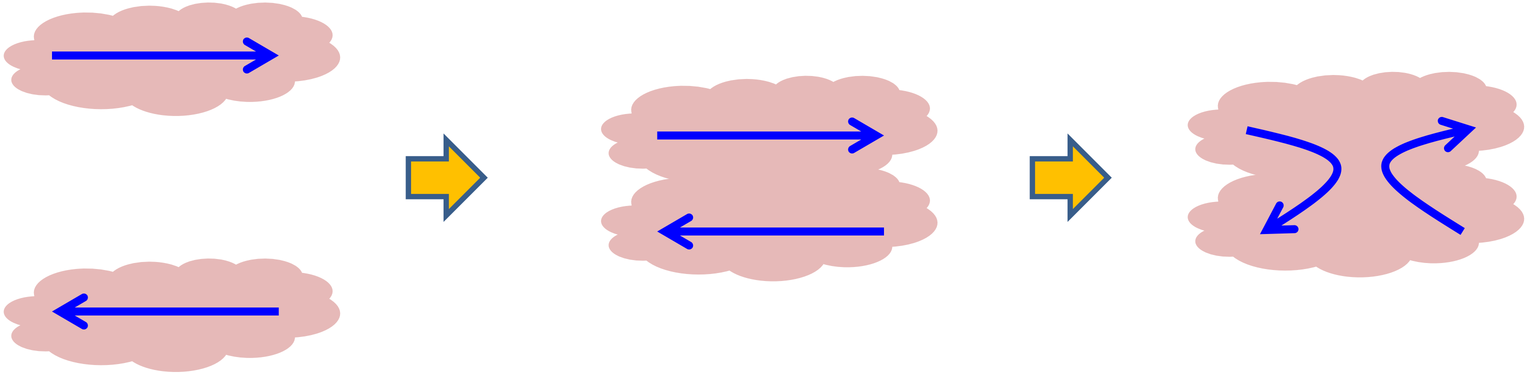

- Magnetic reconnection: two oppositely directed magnetic fields come together and reconnect to change their magnetic topology
  - Happens due to plasma resistivity
  - Converts magnetic energy into particle energy
  - Observed in solar corona, magnetosphere, tokamaks

➢ But details of magnetic reconnection still remain unclear

Details about the Caltech experiment

- Starts with (1) low beta (~ 0.1) → **J**x**B** force is dominant

  (2) large Lundquist number (>10) → flux frozen-in particles
- Visualize multi-scale physics: single fluid, two-fluid (+kinetic scale)

- Plasma characteristics
  - Breakdown voltage: ~ few kV
  - Plasma current: ~ 100 kA
  - Plasma lifetime: < 50 μs
  - Gas: H_2, N_2, Ne, Ar, Kr

  → **Only Ar used in this work**

* Plasma beta: $\beta = nk_BT/(B^2/2\mu_0)$
* Lundquist #: $S = \mu_0 L v_A/\eta$

Formation of plasma jet

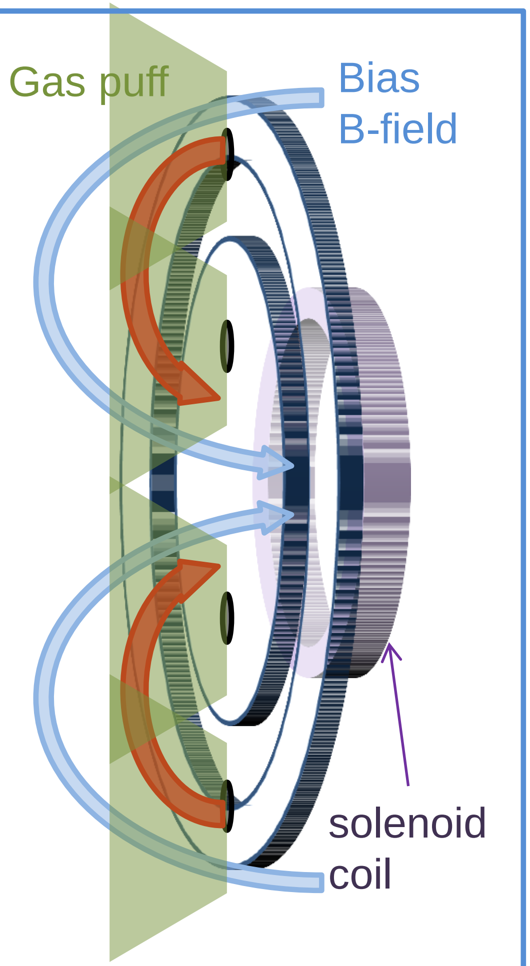

8 plasma-filled flux tubes form along the bias field

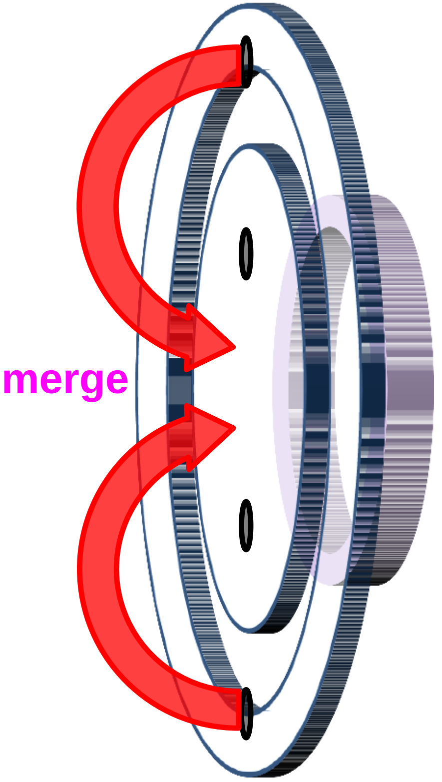

Currents in the same direction attract each other → jet forms

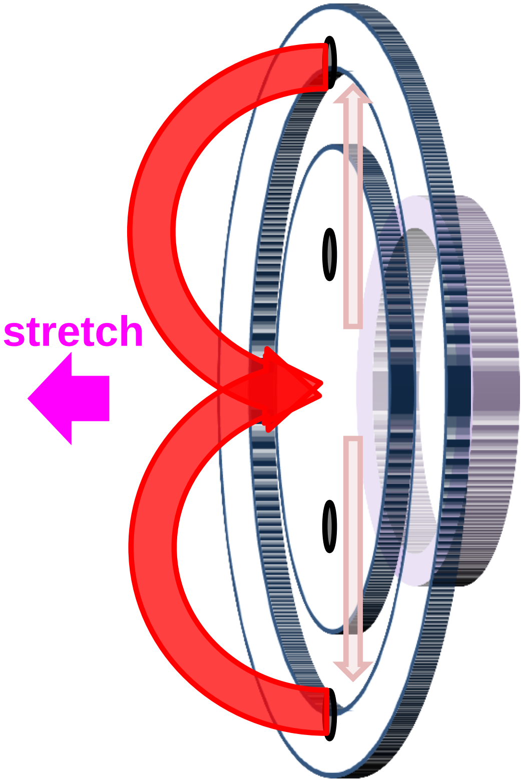

Axial gradient of **J**x**B** force → jet stretches

Ideal-MHD kink instability

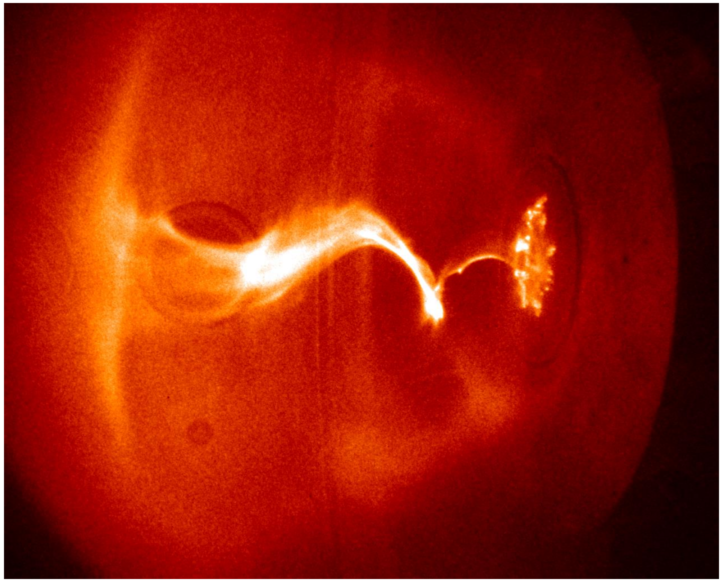

q : measure of pitch of helical magnetic field

- As jet length exceeds a critical value plasma becomes kink unstable
- Can be explained by Kruskal-Shafranov criterion: kink occurs when $q < 1$
  - $q = 2\pi r B_z / L B_\phi$
  - L increases → q decreases

S. C. Hsu and P. M. Bellan, PRL **90**, 215002 (2003).

Rayleigh-Taylor (RT) instability

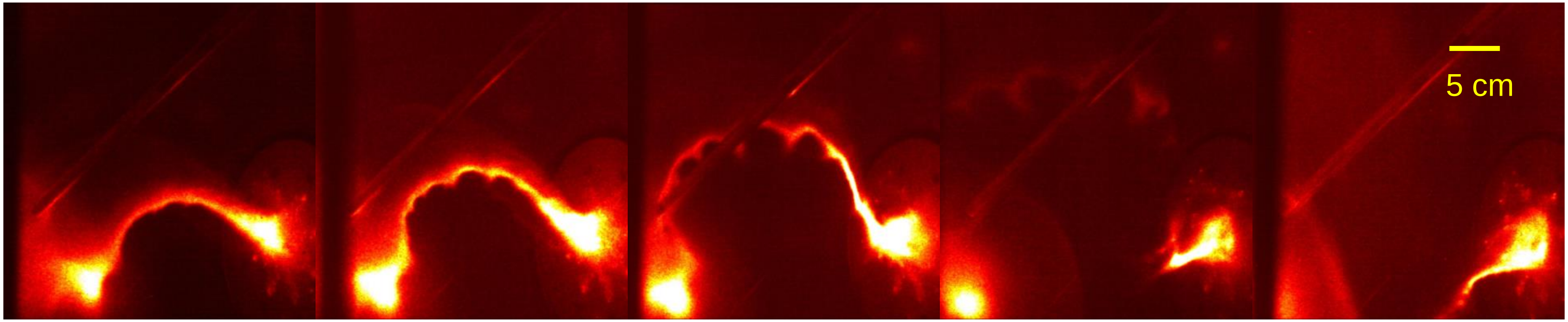

- Kink instability induces effective gravity in the $-r$ direction
- RT instability occurs at interface between heavy plasma and light vacuum
- Finger-like structures: RT ripples
- Plasma diameter pinched by RT ripples to the ion skin depth scale

  → jet becomes in two-fluid regime & Hall physics becomes important
- Drastic change in magnetic topology after RT → magnetic reconnection

Mysterious EUV and RF bursts

- Observe transient EUV bursts & high frequency fluctuations when jet detaches from electrodes:
  - They are conjectured to be associated with magnetic reconnection
- Goal: study details of magnetic reconnection occurring in our jet by using comprehensive diagnostics

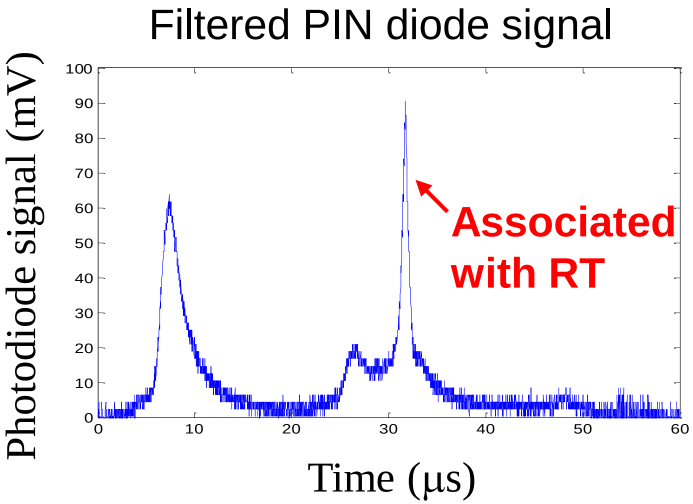
Filtered PIN diode signal

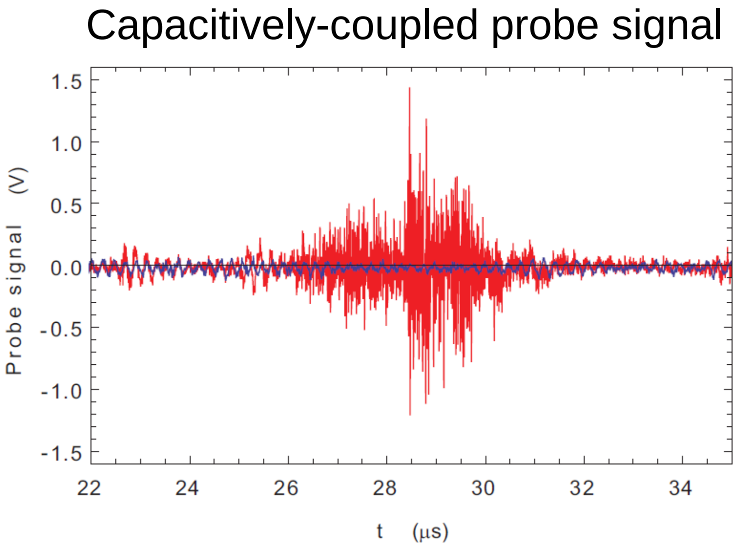
Capacitively-coupled probe signal

Sketch of diagnostics

B-dot probe measures high freq. magnetic fluctuations

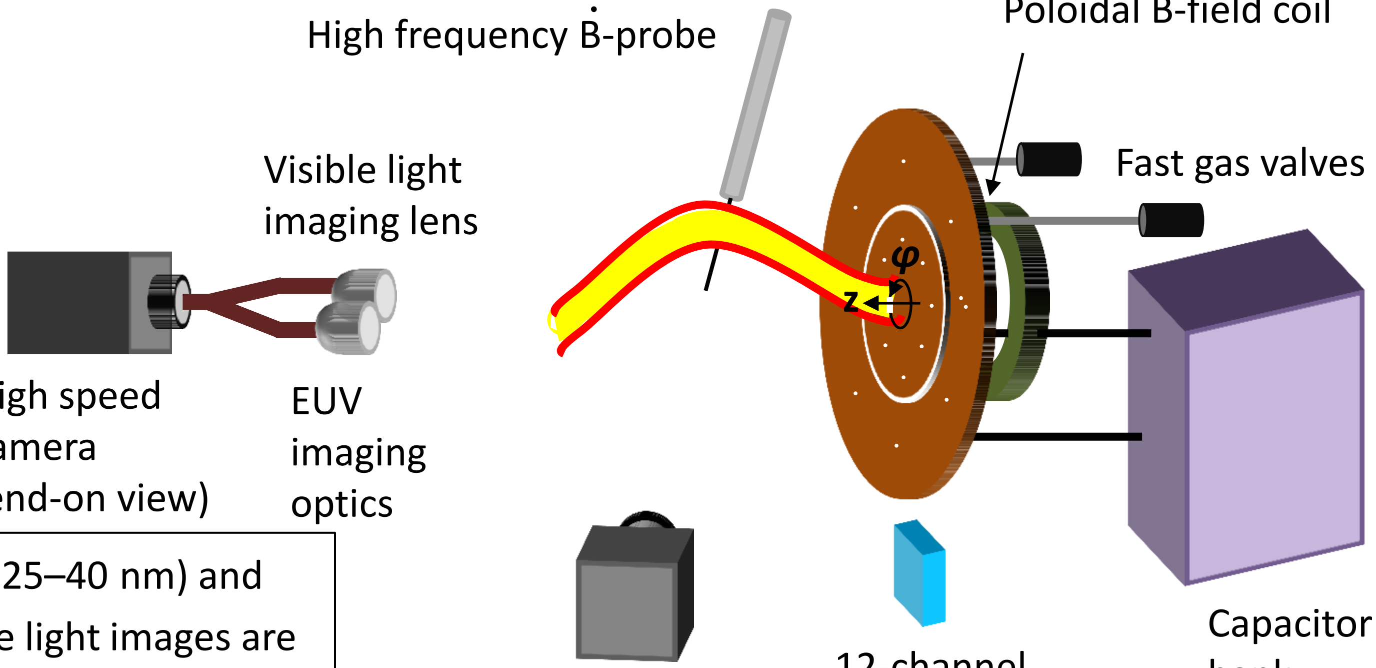

High frequency $\dot{B}$-probe

Poloidal B-field coil

Visible light imaging lens

Fast gas valves

High speed camera (end-on view)

EUV imaging optics

EUV (25–40 nm) and visible light images are simultaneously captured

High speed camera (side view)

12-channel spectroscopic array

Capacitor bank

Spectroscopic system measures Doppler and Stark broadenings

EUV (25–40 nm) vs visible light

End-on view

red: EUV; blue: visible light

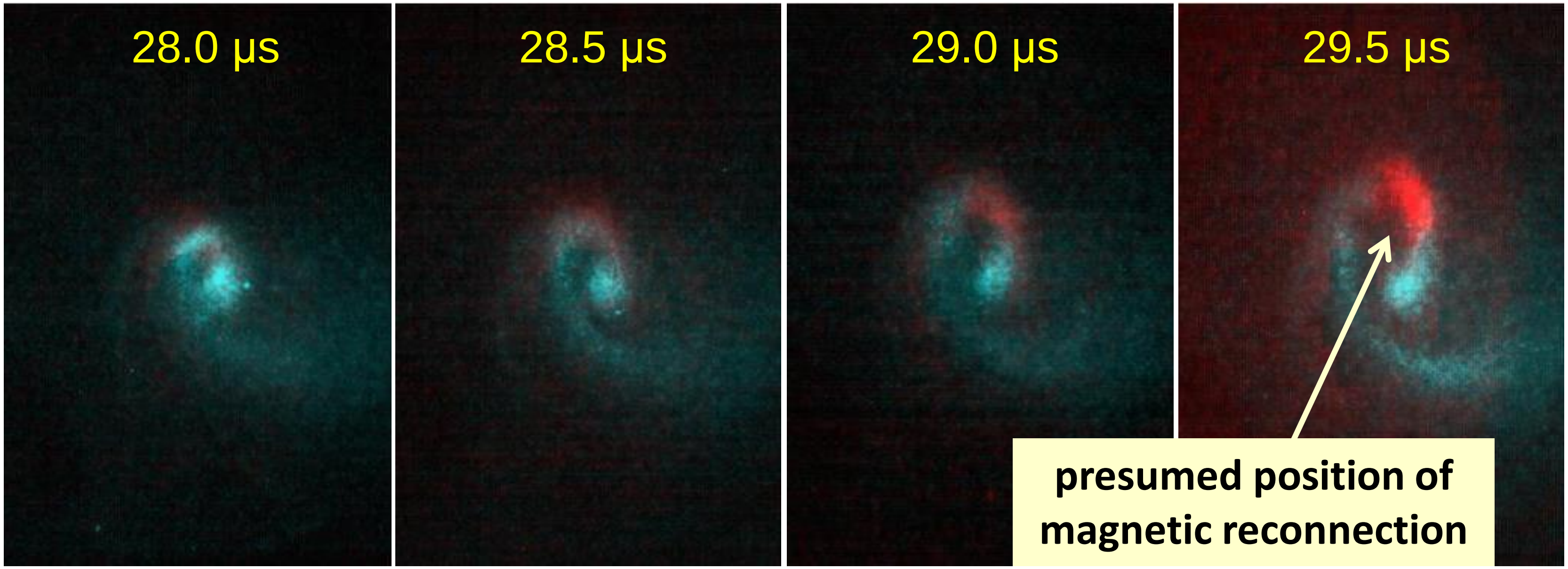

presumed position of magnetic reconnection

- As RT instability grows and reconnection occurs:
  - 25–40 nm EUV (red) becomes extremely bright in localized area
  - Visible light (blue) becomes dark where EUV gets bright
- Ar VI–VIII (Ar^{5+}–Ar^{7+}) lines exist in 25–40 nm

→ Plasma becomes higher ionization state after reconnection (electron heating)

K.-B. Chai, X. Zhai, and P. Bellan, Phys. Plasmas **23**, 032122 (2016).

Plasma emission spectrum

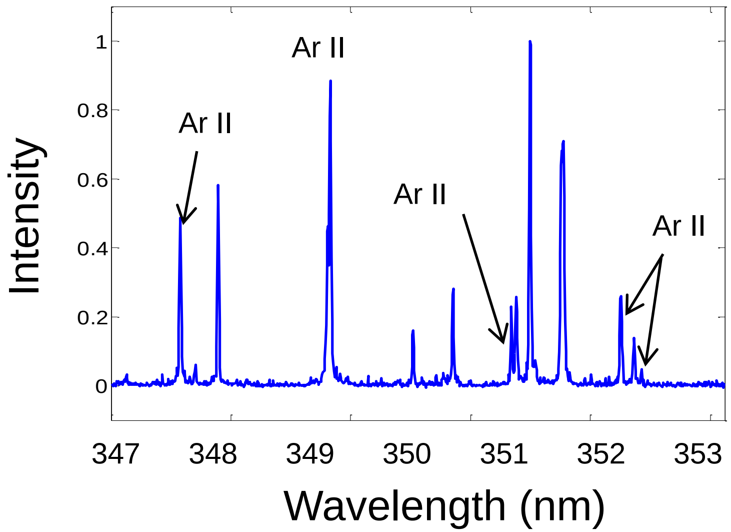
Before RT (@ 20 μs)

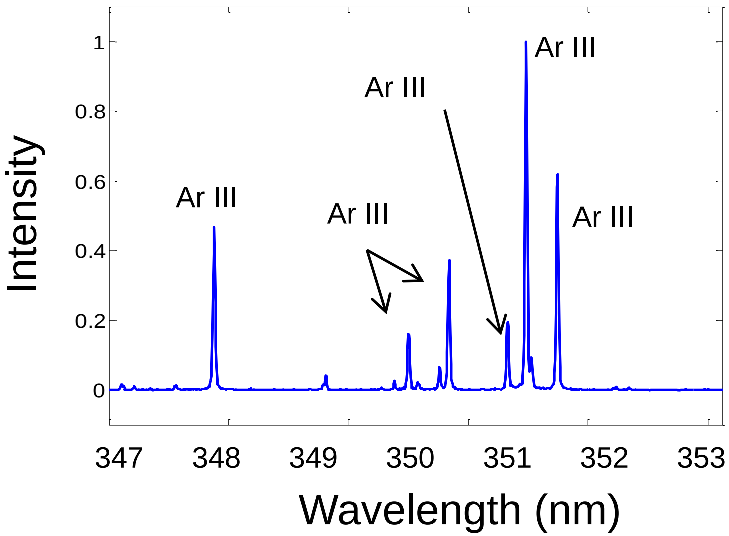
During RT (@ 28 μs)

- As RT instability and reconnection occur:
  - Ar II (Ar^{+}) lines disappear and Ar III (Ar^{2+}) lines dominate over Ar II lines
  - Ar IV (Ar^{3+}) lines are also observed

→ Indicates plasma become higher ionization state and electron heating

Doppler & Stark broadening

Before RT (@ 20 μs)

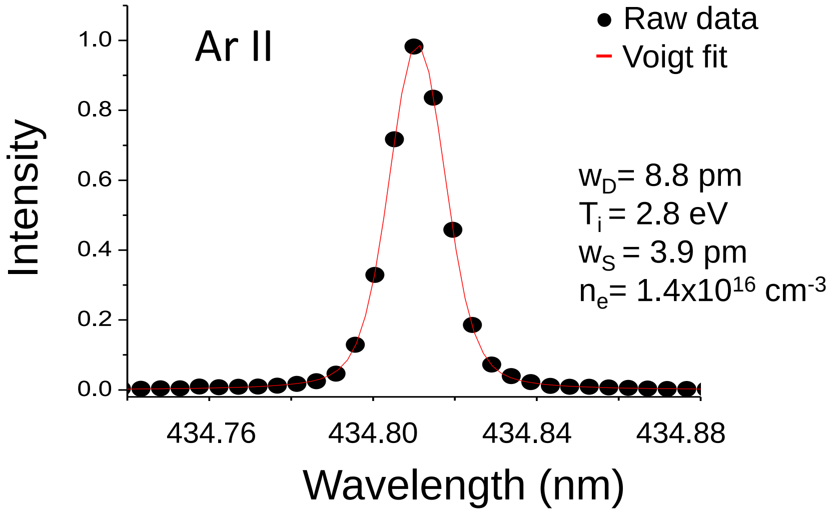

During RT (@ 28 μs)

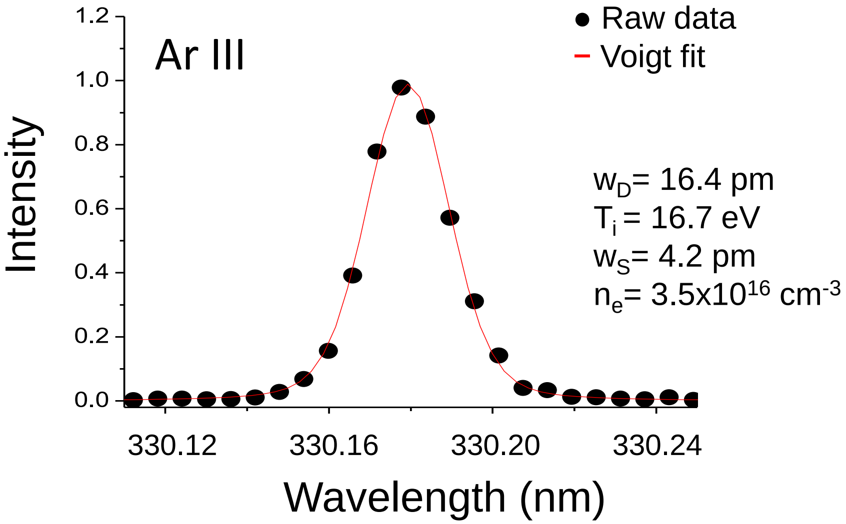

- Voigt function: convolution of Gaussian and Lorentzian
- Voigt fitting gives both Doppler (Gaussian) & Stark (Lorentzian) widths
- As RT and reconnection occur:
  - T_i: 2.6 ± 0.4 eV → 15.8 ± 2.3 eV
  - n_e: (1.6 ± 0.3)×10^{16} cm^{-3} → (5.1 ± 2.1)×10^{16} cm^{-3}

High freq. magnetic fluctuation

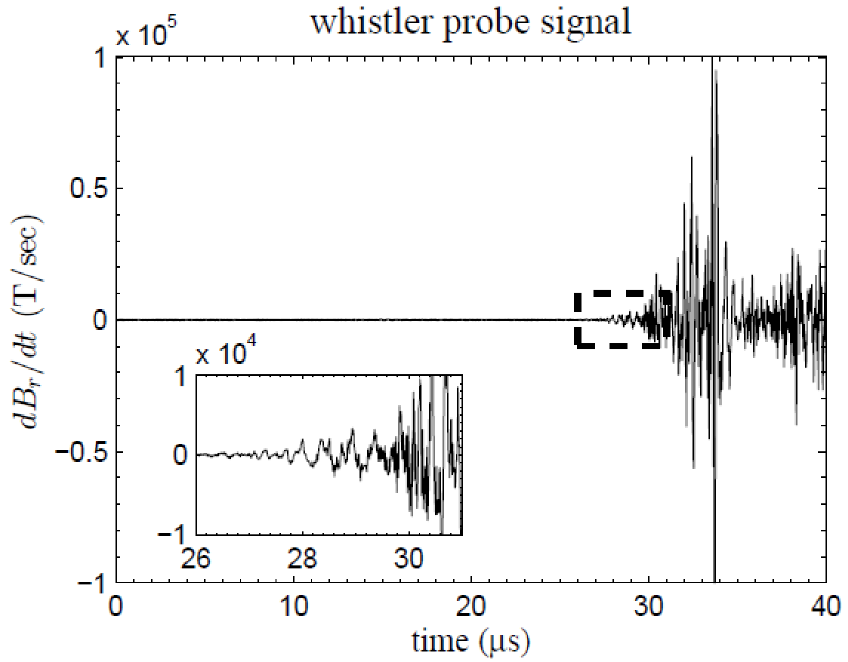
whistler probe signal

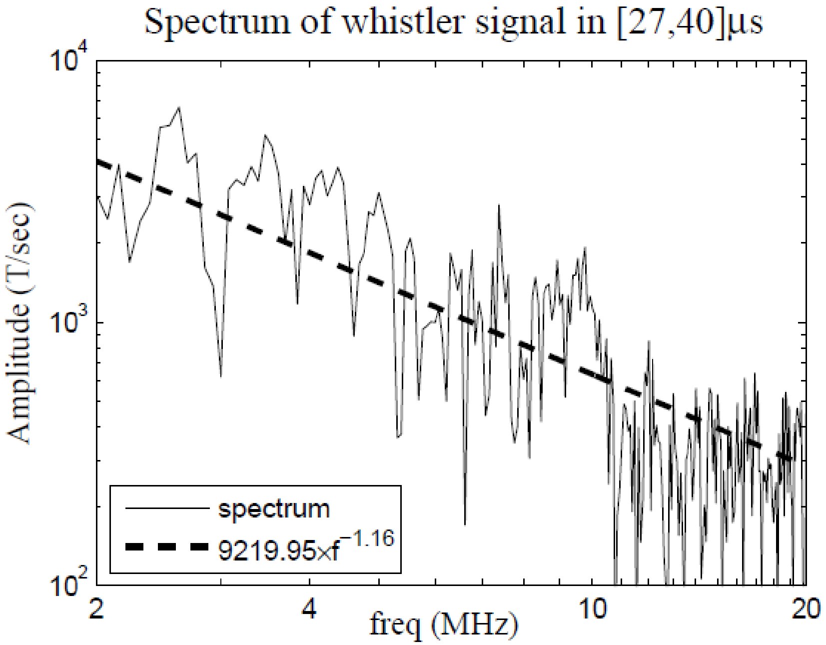
Spectrum of whistler signal in [27,40]µs

- Broadband (2-20 MHz) high frequency magnetic fluctuations observed when EUV burst appears
  - Ion cyclotron freq. < observed wave freq. < electron cyclotron freq.
  - Have power-law dependence on freq. (~ f^{-1}) → but not turbulence

Whistler waves: Circular polarization

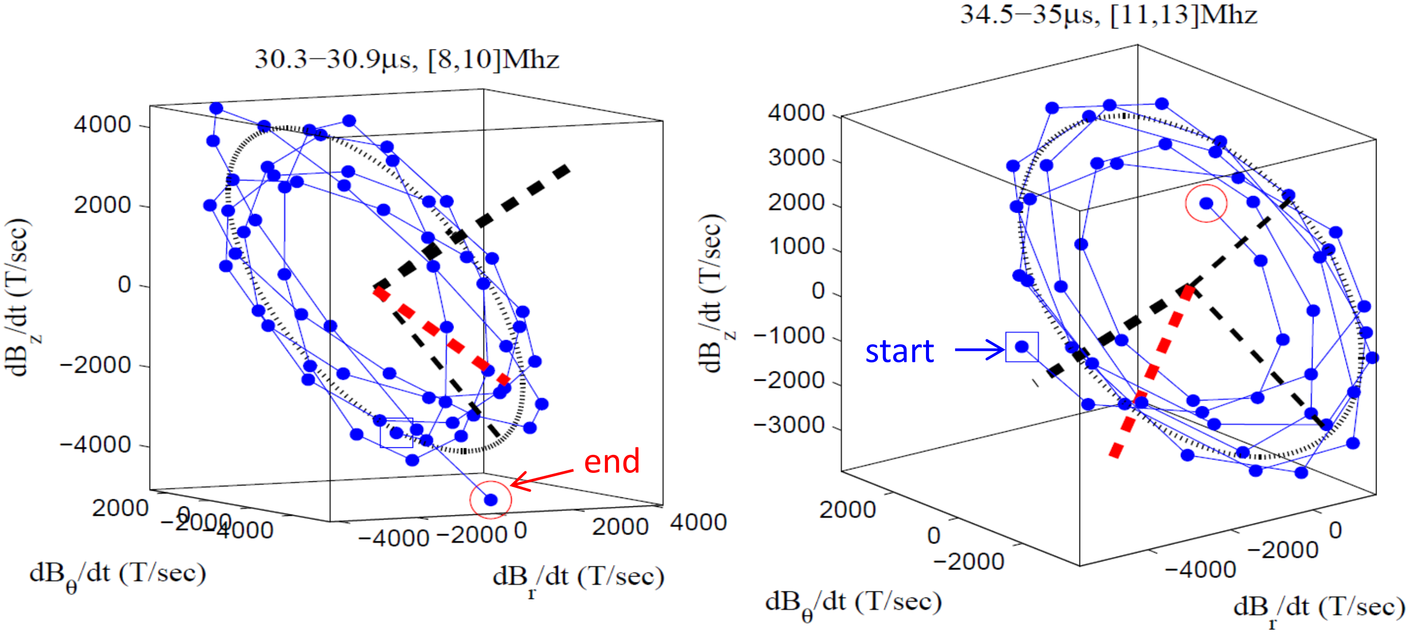

- Hodograms of magnetic vector show circular polarization & oblique propagation
- Whistler waves: circularly polarized B-field even when obliquely propagating*

  → Measured fluctuations are whistler waves
- Whistler wave: Hall-MHD phenomenon → our reconnection is Hall-MHD reconnection

* P. Bellan, Phys. Plasmas **20** ,082113 (2013).

Voltage spikes

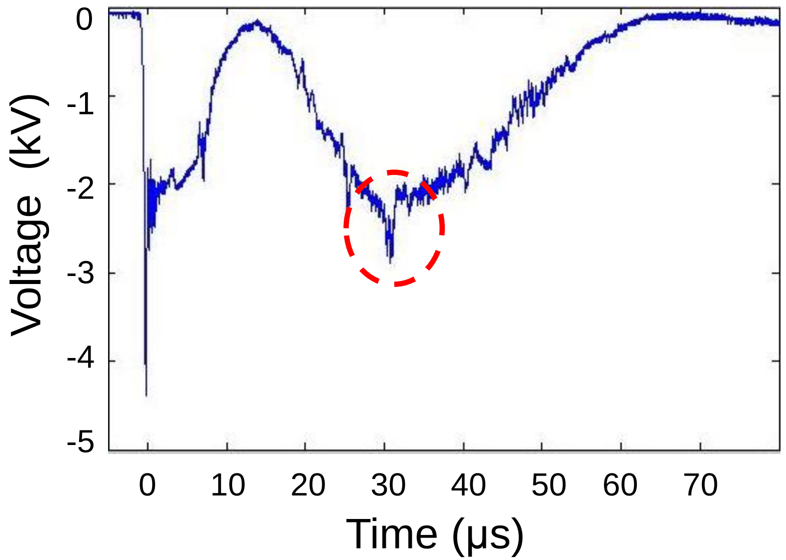

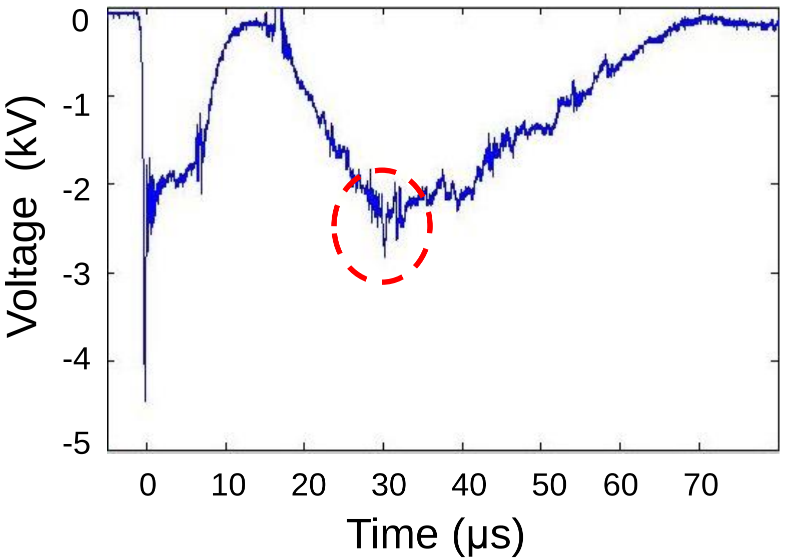

- When EUV burst and whistler waves appear:
  - Reproducible, >500 V voltage spikes lasting ~1 μs appear

→ Results from magnetic reconnection that changes magnetic flux linking the electrode circuit

T_e estimation: FLYCHK

- Before reconnection, plasma jet is in LTE but it is not after reconnection*

  → $T_{e0} = T_{i0}$ = 2.6 eV but $T_{e1} \neq T_{i1}$ (= 15.8 eV)
- Using FLYCHK, the average ionization $\langle Z_0 \rangle = 1.7$ with $n_{e0} = 1.6\times10^{16}$ cm^{-3}

  → $n_{i0} = 9.4\times10^{15}$ cm^{-3}

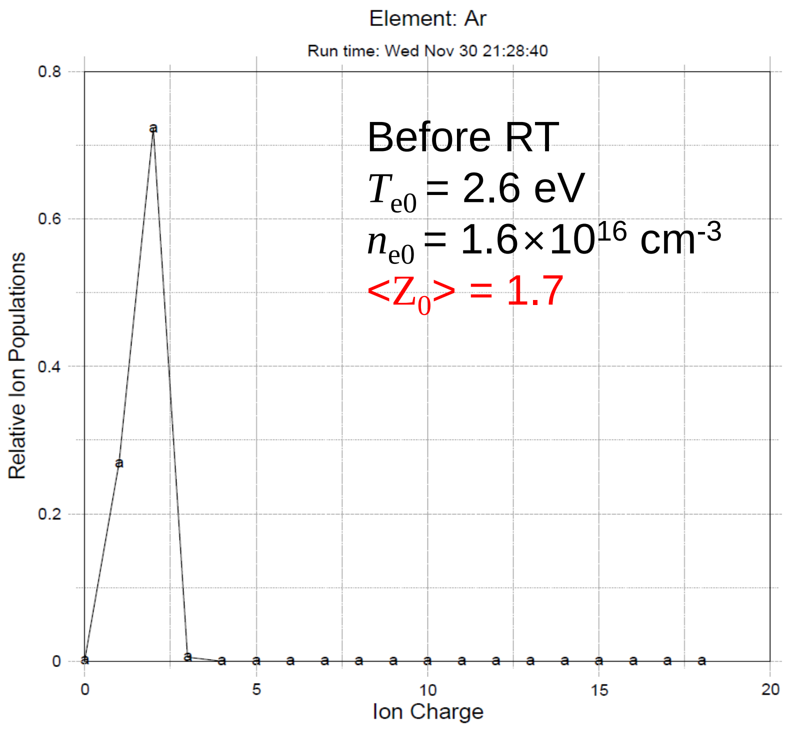

Before RT

T_{e0} = 2.6 eV

$n_{e0} = 1.6\times10^{16}$ cm^{-3}

$\langle Z_0 \rangle = 1.7$

* G. Yun, Caltech PhD thesis (2008)

T_e estimation: FLYCHK

- Assuming no change in ion density after reconnection & using Stark broadening result ($n_{e1} = 3.2\ n_{e0}$) → $<Z_1> = 3.2 \times <Z_0> = 5.5$
- $<Z_1> = 5.5$ can be obtained with T_{e1} = 11 eV & $n_{e1} = 5.1 \times 10^{16}$ cm^{-3} (FLYCHK)

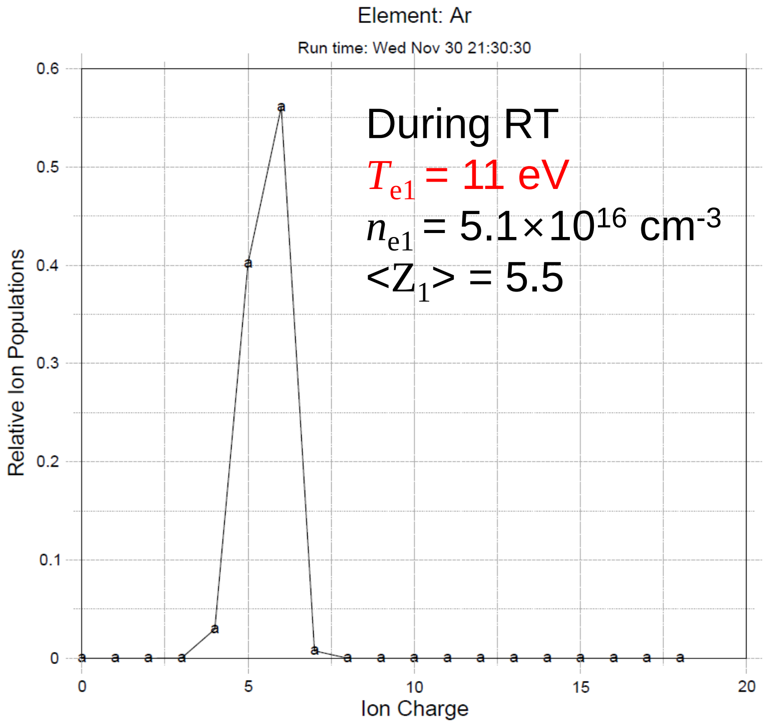

During RT
T_{e1} = 11 eV
$n_{e1} = 5.1 \times 10^{16}$ cm^{-3}
$<Z_1> = 5.5$

	Before reconnection	**After reconnection**
T_e	2.6 eV	11 eV
T_i	2.6 eV	15.8 eV
n_e	1.6×10^{16} cm^{-3}	5.1×10^{16} cm^{-3}
n_i	9.4×10^{15} cm^{-3}	9.4×10^{15} cm^{-3}
$<Z>$	1.7	5.5

Electron Ohmic heating

- Our estimation: T_e increased from 2.6 eV to 11 eV
- Observed electron heating rate:

$$3n_\mathrm{e}\Delta(k_\mathrm{B}T_\mathrm{e}) / 2\Delta t = 1.0\times10^{11}\ \mathrm{Wm^{-3}}$$

- Ohmic heating rate inside current sheet with Spitzer resistivity

$$5.7\times10^{9} < \eta J^2 < 1.1\times10^{13}\ \mathrm{Wm^{-3}}$$

→ Wide range is due to the uncertainty in estimate of J

→ Ohmic heating inside out-of-plane current is likely the cause of observed electron heating

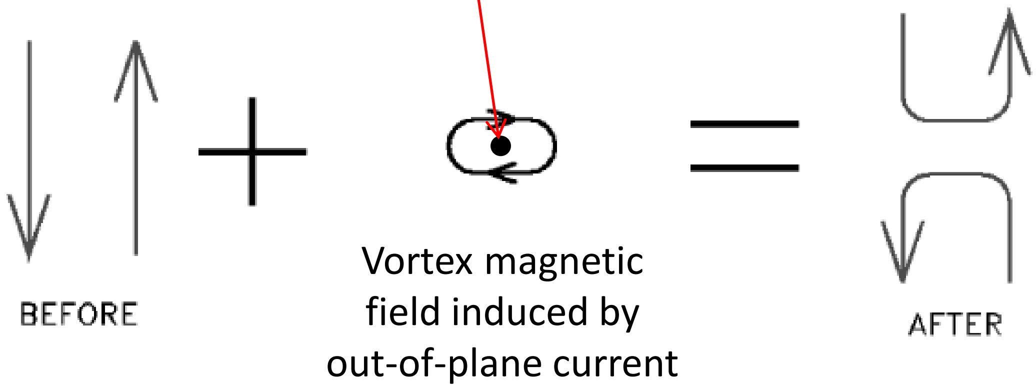

Ion stochastic heating

- Stochastic heating has been proposed
- z component of Generalized Ohm's law:

$$E_z + \hat{z}\cdot \mathbf{U_T}\times\mathbf{B_T} - \hat{z}\cdot \mathbf{J_T}\times\mathbf{B_T}/ne = \eta J_z$$

  - Outside $r >$ ion skin depth, second and third terms are ignorable

$$-\partial\phi/\partial \mathrm{z} - \partial A_\mathrm{z}/\partial t \approx \eta J_z$$

- Ampere's law → $B_\theta=\mu_0 J_\mathrm{z} r/2,\ A_\mathrm{z}=-\mu_0 J_\mathrm{z} r^2/4$
- Transient out-of-plane current $J_\mathrm{z}=J_\mathrm{z0}\mathrm{e}^{-t/\tau}$: τ is reconnection time scale

$$\phi = -\int (\partial A_\mathrm{z}/\partial t + \eta J_z)\,\mathrm{dz}$$

$$E_r = -\partial\phi/\partial r = \mu_0 J_\mathrm{z0}\mathrm{e}^{-t/\tau}\, r\mathrm{z}/2\tau$$

- If E_r is strong so that $m_i(q_i B^2)^{-1}\,\partial^2\phi/\partial r^2 > 1$ is satisfied, ion trajectory becomes stochastic (guiding center approx. breaks down).

Ion stochastic heating

- Using nominal values of B = 0.6 T, z = 2 cm, J_{z0} = 10^8 A/m^2, stochastic condition satisfied if τ < 3 μs.
- Observed τ = 1 μs → our jet is in the stochastic regime.
- Trajectory of ions calculated by numerically integrating Lorentz Eq. with previously shown $\mathbf{E}$ and $\mathbf{B}$ confirms our argument.

τ =100 μs (below criterion)

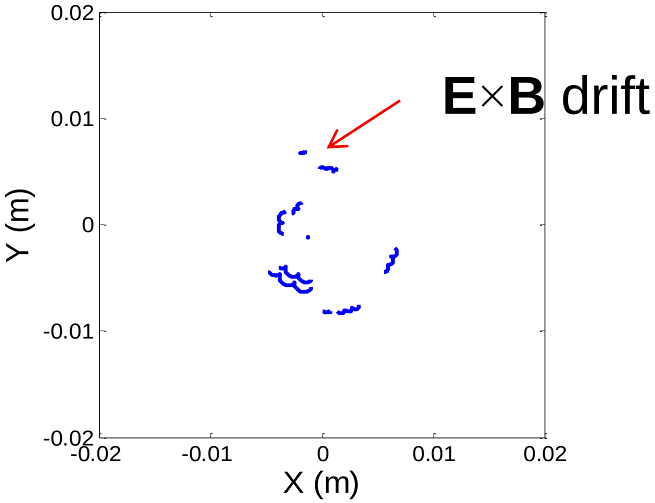

τ =1 μs (above criterion)

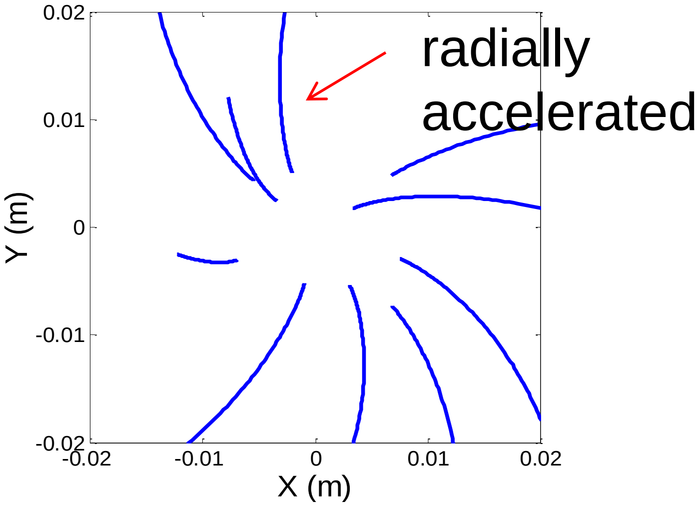

Summary

- Observations:
  - Magnetic reconnection associated with Rayleigh-Taylor instability occurs
  - Jet diameter pinched to ion skin depth and Hall term becomes important
  - Strong, transient EUV burst (electron heating)
  - Doppler broadening in plasma emission lines (ion heating)
  - Whistler wave emissions (Hall-MHD physics)
  - Voltage spike (sudden change in magnetic topology)
- Discussion:
  - Electron heating is likely caused by Ohmic dissipation
  - Ion heating plausibly results from stochastic heating